Receptor−Ligand Binding in the Cell−Substrate Contact Zone: A Quantitative Analysis Using CX3CR1 and CXCR1 Chemokine Receptors†

Fang-Hua Lee,‡ Christopher Haskell,§ Isreal F. Charo,|| and David Boettiger‡,⊥,*

Departments of Microbiology and Pharmacology, University of Pennsylvania, Philadelphia, Pennsylvania 19104, Berlex Biosciences, Richmond, California 94806, and Gladstone Institute, University of California, San Francisco, San Francisco, California 94141

Received December 9, 2003; Revised Manuscript Received March 1, 2004

ABSTRACT: Receptor−ligand binding analyses have generally used soluble components to measure thermodynamic binding constants. In their biological context, adhesion receptors bind to an immobile ligand and the binding reaction is confined to the cell−substrate contact zone. We have developed a new procedure based on the spinning disk technology to measure the number of receptor−ligand bonds in the contact zone. Application of this methodology to the CX3CR1−fractalkine and the CXCR1−IL-8 receptor−ligand systems demonstrated that the level of binding to an immobilized ligand is reduced by several orders of magnitude in comparison to solution binding. A comparison of the solution binding and contact zone binding constants shows that the effect of ligand immobilization was similar for each system. In contrast, although the CXCR1−IL-8 bond had the higher affinity, the average bond strength was only 10% of that for the CX3CR1 bond. Because fractalkine can be expressed as a cell surface-bound protein, CX3CR1 has been proposed to function as an adhesion receptor. The higher bond strength suggests that the bond architecture has also evolved to serve an adhesion function.

Cell adhesion involves the interaction of cell surface receptors with counter receptors or ligands displayed either on other cells or as an extracellular matrix. For stable cell adhesion, these reactions may involve thousands of receptor−ligand bonds. These receptor−ligand bonds are formed in a cell−substrate space that we shall call the contact zone. The constraints on the interactions between receptor and ligand in the contact zone are different from those in which soluble ligands bind to cell surface receptors on cells in suspension. The relationship between the equilibrium dissociation constants derived for the case of the soluble ligands, which we shall call the K_{3D} (three-dimensional space), and those in the contact zone, which we shall call K_{2D} (two-dimensional space), remains to be determined. For cell adhesion, K_{2D} is likely to be the significant parameter.

Two general approaches have been used to measure receptor−ligand binding in the contact zone. Dustin et al. (*1*) analyzed LFA-3−CD2 binding in the contact zone by adding CD2-expressing cells to lipid bilayers containing different densities of fluorescent-labeled LFA-3. The proportion of bound receptors was determined from the distribution of LFA-3 into the contact zone. This fluorescent method has been extended to other receptor−ligand pairs (*2*, *3*). This analysis depends on the assumption that all of the receptor−ligand pairs can be formed in the contact area where the fluorescence concentrates are formed and that dissociation results in the rapid exit of the labeled molecule from the complex. The second approach uses mechanical forces. Most of the available data has been developed for the binding of selectins to substrate-attached ligands in a flow chamber (*4*−*6*). Analysis of the transient rolling and release was used to calculate on and off rates. Alternatively, manipulating cells into and out of contact with an adhesive substrate using a micropipet provides an alternative strategy for making the same measurements (*7*, *8*). In these analyses, the K_{on} is determined from the probability of bond formation and the K_{off} is determined from the duration of the bond. Analyses of P- and E-selectin have also been made using the plate centrifugation method to separate cell and substrate (*9*). Interestingly, the values for K_{2D} obtained using the different mechanical force measurements were similar (10^5−10^7 $\eta/\mu m^2$) (*2*) and contrasted with values for K_{2D} in the range of 1−10 $\eta/\mu m^2$ using the fluorescence methods. Thus, assuming a cell−substrate separation distance of 10−20 nm, the values for K_{2D} using the fluorescent measurements are close to those expected based on the K_{3D} measurements, but the values of K_{2D} for the mechanical measurements were 4−5 orders of magnitude higher than expected from the K_{3D} measurements (*2*). Whether the discrepancy is due to the use of IgG superfamily adhesion molecules for the immunofluorescent analyses and selectins for the force measurements or to differences in the assumptions inherent in the different methods is not clear.

At this time, the force measurements have been limited to cases in which one or a small number of bonds was

† This research was supported by grants HL 63894 (to I.F.C.), CA16502, and GM53788 (to D.B.) from the National Institutes of Health and by a grant from the University of Pennsylvania Research Foundation.

* To whom correspondence should be addressed. Tel: 215-898-8792. Fax: 215-898-9557. E-mail: boettige@mail.med.upenn.edu.

‡ Department of Microbiology, University of Pennsylvania.

§ Berlex Biosciences.

|| Gladstone Institute, University of California.

⊥ Department of Pharmacology, University of Pennsylvania.

10.1021/bi0362121 CCC: $27.50
Published on Web 05/14/2004

involved in binding the cell to the substrate. Because the stable adhesion of a cell to a substrate generally involves a large number of bonds, it is important to have an approach that can be used for those cases. A spinning disk device was developed, which applies a linear hydrodynamic shear gradient to a cell population (*10*). The mean shear stress required to detach the cells is directly proportional to the number of receptor−ligand bonds that attach the cell to the substrate (*11*). Therefore, this method provides a means to determine the relative number of bonds formed in the contact zone. This approach is analogous to the plate centrifugation assay in which force is also used to detach cells (*12*). For the purposes of this report, the spinning disk method offers two advantages. First, it has been more extensively characterized (*11*, *13*, *14*). Second, a higher force can be applied to cause cell detachment making it more suitable for the analysis of cases in which a large number of bonds attach the cell to the substrate.

Previous analyses of 2D binding have been focused on adhesion molecules. Adhesion molecules are subject to various forms of regulation by the cell intent on regulating its adhesion and thus add additional layers of complexity to the analyses. For these studies, we chose to use the seven transmembrane G-protein-associated cell surface receptors CX3CR1 and CXCR1 (*15*, *16*). The ligand for CX3CR1 is FKN.[1] FKN is expressed as a transmembrane protein with a mucin-rich extracellular stalk that presents the receptor binding domain (*17*, *18*). Receptor−ligand binding has been shown to arrest cells from flow in experimental systems. Hence, this bond can function as an adhesive bond and be analyzed using the spinning disk method. The ligand for CXCR1 is IL-8, which is normally expressed as a soluble molecule. The receptor binding domain of IL-8 was substituted for the receptor binding domain of FKN. This permitted the analysis of CXCR1−IL-8 binding under the same conditions as the CX3CR1−FKN binding. These "adhesion receptor" systems also avoid the issues of adhesion receptor signaling present for other adhesion receptors since mutations in the signaling domain do not affect the ligand binding reaction (*19*, *20*, and unpublished data using the spinning disk). Chemokine receptors do undergo a desentization process; however, this does not appear to affect ligand binding itself and hence is not likely to be a complicating factor for the analysis (*21*).

MATERIALS AND METHODS

Cells and Ligands. Murine pre-B cell lines (300-19, 300-19 mCX3CR1, and 300-19 hCXCR1) were cultivated in RPMI-1640 medium (GIBCO BRL, Gaithersburg, MD) supplemented with 10% fetal calf serum (Hyclone Laboratories, Logan, UT), 50 μM β-mercaptoethanol, penicillin (100 IU/mL), and streptomycin (100 μg/mL). DNA constructs for chemokine receptors with N-terminal FLAG epitope and transfection procedures were described in ref (*20*). Stably transfected cells were maintained in the presence of 400 μg/mL G418. Human IL-8−stalk−6-His and human FKN−stalk−6-His have been described previously (*22*). These constructs were used by R & D Systems (Minneapolis, MN) to produce purified proteins.

Fluorescence-Activated Cell Sorter (FACS) Analysis. Relative expression levels of the chemokine receptors on cell surfaces were determined by flow cytometry. Cells were harvested, resuspended at 5×10^6/mL in FACS buffer (0.05 M Tris, 0.15 M NaCl, 1 mM $CaCl_2$, 0.1% bovine serum albumin (BSA), and 0.02% NaN_3, pH 7.4), and then incubated with saturating concentrations of anti-FLAG M1 monoclonal antibody (mAb) (Sigma, St. Louis, MO) for 45 min at 4 °C. The cells were washed, followed by binding fluorescein isothiocyanate (FITC)-conjugated anti-mouse IgG (Jackson ImmunoResearch Laboratory, West Grove, PA) for 30 min at 4 °C. The cells were washed and analyzed on a FACScan (Becton Dickson, San Jose, CA).

Ligand Adsorption (Substrate Preparation). Glass coverslips (25 mm diameter, Bellco Glass Inc., Vineland, NJ) cleaned with 95% ethanol and distilled water were coated with 0.1 mg/mL collagen (type I, Collagen Biomaterials, Palo Alto, CA) and dried overnight. Each coated coverslip was placed on a pedestal (15 mm diameter coverslip) in a 35 mm Petri dish, topped with 300 μL of nitrocellulose (Micron Separations Inc., 1 cm^2/mL methanol), and then air-dried. Right before the cell detachment assay, the treated coverslips were sequentially loaded with 300 μL of anti-hexa-Histidine (6-His) mAb (10 μg/mL, R & D Systems) for 30 min, blocked with 1 mL of 1% heat-inactivated (HI) BSA for 30 min, and then layered with 300 μL of carboxyl-terminal 6-His-tagged FKN or IL-8−mucin stalk chimera (R & D Systems) for 60 min at room temperature. Phosphate-buffered saline (PBS) was used to wash coverslips between each substrate loading.

Cell Detachment Assay. Cell adhesion was measured using a spinning disk device as previously described in ref (*11*). Briefly, cells were harvested, washed, and resuspended in adhesion buffer (24 mM HEPES, 137 mM NaCl, 2.7 mM KCl, 1 mM $MgCl_2$, and 2 mM glucose, pH 7.4). For each assay, 2×10^5 cells in a total volume of 400 μL were evenly seeded onto a ligand-coated glass coverslip mounted on the spinning disk device and allowed to attach for 15 min (unless specified otherwise). After incubation, the chamber of the spinning disk device was carefully filled with adhesion buffer and the cells were spun for 5 min at a constant speed with controlled acceleration rates. After spinning, adherent cells were fixed in 3.7% formaldehyde, permeabilized with 1% Triton X-100, and stained with ethidium homodimer (Molecular Probes, Eugene, OR). The coverslips were analyzed by counting the number of nuclei per microscope field (0.5 mm^2) using an Optiphot fluorescent microscope (Nikon, Garden City, NY) equipped with a motorized Ludl XYZ stage, a filter wheel/shutter (LUDL Electronics Products Ltd., Hawthorne, NY), and a Photometrics SenSys cooled charge-coupled device camera (Tucson, AZ). Sixty-one fields per coverslip were analyzed by Image-Pro V3.0 (Glenn Mills, PA), and the shear stress corresponding to 50% cell detachment (τ_{50}) was calculated by fitting the data to a sigmoid curve by SigmaPlot (SPSS Science, Chicago, IL).

Analysis of Radioligand Binding to Anchored Substrate. Cleaned glass coverslips (9 mm × 9 mm) were coated with collagen and then placed on 5 mm diameter pedestals. The coverslips were layered with 50 μL of nitrocellulose and air-dried. Immediately before the binding experiment, treated

[1] Abbreviations: FKN, fractalkine; FACS, fluoresence-activated cell sorting; τ_{50}, mean shear stress for cell detachment; L, ligand density; R_B, number of bound receptors per cell; *RT*, universal gas constant times absolute temperature.

coverslips were sequentially coated with 50 μL of anti-6-His mAb (10 μg/mL) for 30 min, washed once with PBS, blocked with 200 μL of 1% HI-BSA for 30 min, washed once with PBS, and then loaded with 50 μL of a combination of Bolton−Hunter labeled ^{125}I-6-His-tagged FKN and varying concentrations of unlabeled FKN. After they were incubated at room temperature for 1 h, the coverslips with bound FKN were washed with PBS and then scanned with Wallac WIZARD Automatic Gamma Counter (PerkinElmer Life Sciences, Boston, MA). Anti-6-His mAb was replaced by BSA for nonspecific binding at each ligand concentration.

Analysis of Receptor Binding to Soluble Ligand. Murine CX3CR1 or human CXCR1-transfected 300-19 cell lines were harvested, washed, and resuspended in adhesion buffer + 1 mg/mL BSA + 0.01% sodium azide. The binding assays were conducted in a total volume of 200 μL, consisting of 100 μL of cell suspension (10^6 cells), 50 μL of a combination of Bolton−Hunter labeled ^{125}I-chemokine, varying concentrations of unlabeled chemokine, and 50 μL of buffer. Recombinant chemokines obtained from R & D Systems containing both the stalk and the 6-His tag exactly as used for the adhesion analyses were used for the soluble ligand binding experiments. After the chemokines were incubated for 90 min at room temperature under gentle agitation, 50 μL aliquots were layered in triplicate onto 300 μL of 20% sucrose gradient in 0.4 mL microcentrifuge tubes. The bound chemokine was separated from the unbound chemokine by centrifugation at 12 000*g* for 3 min, and the tips of the tubes containing the cell pellet were clipped and quantified. The nontransfected cell line (300-19) was used for nonspecific binding. All radioligand binding data were analyzed using rectangular hyperbola regression for monovalent receptor−ligand binding provided by SigmaPlot.

RESULTS

Principle of the Analysis. To develop a model for the analysis of the CX3CR1−FKN bond, CX3CR1 was transfected into the 300-19 lymphocyte cell line. The FACS analysis in Figure 1A shows that the cell surface expression of CX3CR1 was detected with a narrow range of expression levels, which could be used for the spinning disk analysis. The transfected cells were plated on FKN-coated coverslips and analyzed using the spinning disk. Figure 1B shows the analysis of a typical spin. Each of the points represents a normalized cell density taken at a fixed radial position from the axis of rotation. On the basis of the calibration of the hydrodynamic shear stresses for the apparatus, a surface shear stress was calculated for each radial position (*X*-axis). The data were fit to a sigmoid curve based on the assumption that the mean cell detachment shear stress was a normally distributed cell property. It is expected to vary with both variations in cell size and variations in receptor density. From the curve fit, a τ_{50}, or mean cell detachment, shear stress was determined. Although shear stress is not the same as force applied to detach the cell, as long as the cell sizes and shapes are similar, the proportionality between shear stress and applied force will not vary. Figure 1C shows that for low ligand densities, increasing the density produced a proportional increase in τ_{50}. According to the laws of chemical equilibrium, the number of bonds that form should be directly proportional to receptor and ligand density. Because τ_{50} was also directly proportional to ligand density,

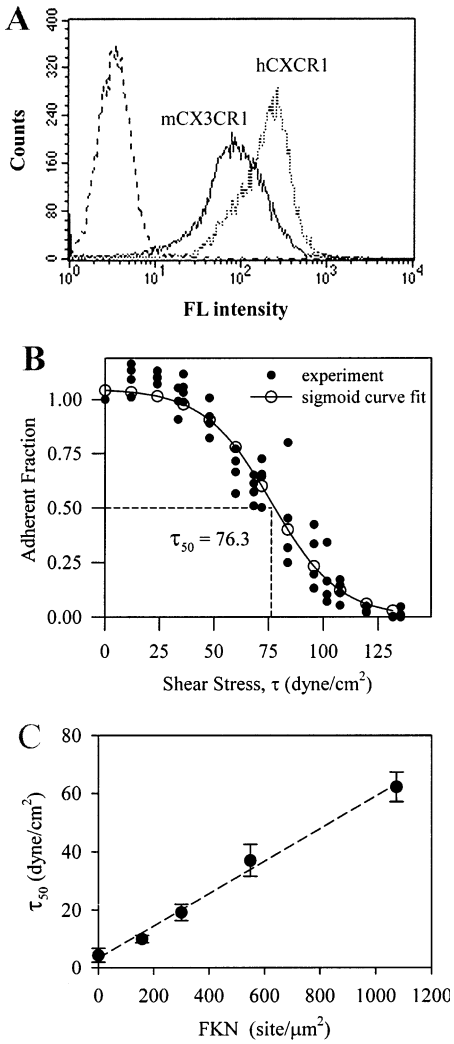

FIGURE 1: Analysis of chemokine-mediated adhesion strength by cell detachment assay. (A) Flow cytometric analysis of chemokine expression using anti-FLAG M1 mAb to detect the N-terminal FLAG tag on the chemokine constructs. Nontransfected 300-19 cells (dash line), 300-19 transfectants expressing mCX3CR1 (solid line), and hCXCR1 (dotted line). (B) Characteristic cell detachment profile; shown is a fraction of adherent mCX3CR1-transfected 300-19 cells as a function of surface shear stress (τ) on a collagen/nitrocellulose-treated coverslip coated with 0.5 μg/mL 6-His-tagged FKN. The adherent fraction is the cell density normalized to the center of the disk. Curve fit parameters: $\tau_{50} = 76.3$ dyne/cm^2, $R^2 = 0.94$. (C) Linear relationship between CX3CR1-mediated cell adhesion strength (τ_{50}) and FKN density at lower ligand densities (<1100 sites/μm^2). Error bars indicate the standard errors ($n = 3$). The dashed line represents linear regression, $R^2 = 0.99$.

it provides a direct measure of the relative number of receptor−ligand bonds.

Most analyses of receptor−ligand binding are based on the model of the law of mass action (ligand + receptor ←ThinSpace→ ligand:receptor). The model assumes that binding occurs as a result of random receptor−ligand associations, that the binding reaction is reversible, and that equilibrium is reached when the binding and unbinding reactions are equal. This leads to the equation for determining the number of bound receptors:

$$R_B = B_{max}L/(K_D + L) \quad (1)$$

R_B is the number of bound receptors (per cell); B_{max} is the total number of receptors per cell available for binding; L is

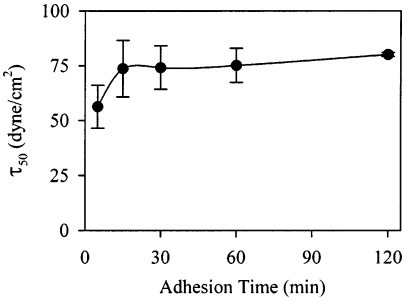

FIGURE 2: FKN-mediated adhesion strength as a function of adhesion time. The same densities of mCX3CR1-transfected 300-19 cells (400 cells/mm^2) are seeded on the coverslips coated with 0.5 μg/mL 6-His tagged for various amounts of time. Error bars indicate the standard deviation ($n = 3$).

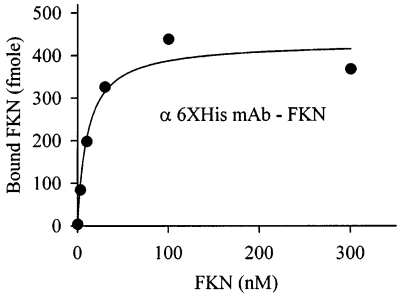

FIGURE 3: Quantitative analysis of chemokine ligand density on the coverslip for cell detachment assay. Shown are the binding characteristics of ^{125}I-FKN to a anti-6-His antibody/nitrocellulose-coated surface. Nonspecific binding, determined by the binding of ^{125}I-FKN to the BSA/nitrocellulose-coated surface, was subtracted. The parameters derived from a rectangular hyperbola regression for monovalent receptor−ligand binding were as follows: $K_D = 11.1 \pm 3.5$ nM, maximum ligand density $= 3.2 \pm 0.2 \times 10^3$ sites per μm^2, $R^2 = 0.96$, $n = 3$.

the ligand density; and K_D is the equilibrium dissocation constant. By varying the ligand density , measuring R_B, and fitting the data to the curve generated by eq 1, the values for B_{max} and K_D can be determined. This approach can be adapted for the analysis of data developed by the spinning disk analysis. First, the analysis does not determine R_B but a τ_{50} measurement that is proportional to R_B. This also means that the value obtained for B_{max} from the curve fitting is a complex constant including factors for cell shape and bond strength. However, because we are not concerned with these issues here, these conversions will be represented by the single constant (C). Second, a value for ligand density (N_L) is substituted for ligand concentration (L) and the 2D dissociation constant (K_{2D}) is used. Thus:

$$\tau_{50} = CN_L/(K_{2D} + N_L) \quad (2)$$

By fitting the data for τ_{50} as a function to N_L to eq 2, it is now possible to determine a value for K_{2D}, provided that the conditions of dissociation and equilibrium are met.

Analysis of Equilibrium. On a 300-19 cell in suspension, the CX3CR1 receptors are likely to be randomly distributed on the cell surface and the ligands will be randomly distributed on the substrate surface. The contact between the two surfaces may align a few receptor−ligand pairs within sufficient physical proximity to bind, but this will be a very small proportion of the total. Although the ligand is bound to a spot, the receptors will be able to diffuse within the plane of the membrane. Thus, it is expected that it will take some period of time for the system to reach an equilibrium state in terms of the number of receptor−ligand bonds. CX3CR1-transfected 300-19 cells were plated on a FKN substrate and assayed using the spinning disk at different times after plating. Because the assay measures the proportion of cells that are retained at each shear stress as compared to the cells at minimum shear stress (at the center of rotation), it corrects for the rate of cell settling. Figure 2 shows an initial rise in τ_{50} to reach a steady state by 15 min after plating. From 15 to 120 min, there was no significant change in τ_{50}. This demonstrates that equilibrium binding conditions were achieved by 15 min after plating.

Determining Ligand Density. Because the ligand has been immobilized, the presentation of ligand on a surface is more complex than presenting ligand in solution. Only ligands that are presented in a form in which the receptor binding site is exposed and available to the receptor and which are not altered by the interaction of the ligand with the solid substrate can be counted. For the spinning disk analysis, there is the additional requirement that the ligand be sufficiently bound to the substrate that it is not released when force is applied through the bound receptor. Nonbiological surfaces, including glass and polystyrene used for culture dishes, have considerable propensity to denature or alter bound proteins (*23*−*26*). Thus, it was important to insulate FKN from the nonbiological surface. A FKN construct was made in which the transmembrane and cytoplasmic domains were replaced with a 6-His tag. The glass surfaces were coated first with collagen and then nitrocellulose. The collagen was necessary to keep the nitrocellulose in place during spinning because the nitrocellulose provides strong binding for the proteins. The nitrocellulose was then coated with anti-6-His antibody. To test this combination, coverslips with this coating were incubated with ^{125}I-FKN (6-His recombinant). Figure 3 shows the binding plot. The saturation level for FKN binding was 3.2×10^3 molecules/μm^2. For immunoglobin with a molecular mass of 160 kDa, it would have a globular protein size of ~10 nm diameter; this would give a monolayer of 10^4 IgG/μm^2. If the IgG binds in a random orientation, then one-sixth will be approximately binding side-up and each has two binding sites, which gives 3.3×10^3 binding sites/μm^2, in good agreement with the measured value. The FKN is presented on an oriented stalk in a protein context. The curve fit of eq 1 to the plot shown in Figure 3 generates a K_D value of 11.1 nM. This equation can now be used to calculate the density of bound FKN for each concentration added to the substrate. Because the IL-8 construct has the same stalk and antibody binding region, the data can also be applied to the calculation of the bound density of the FKN−stalk−IL-8 receptor.

Quantitative Analysis of the 2D Binding Affinity Constant for CX3CR1. The specificity of the CX3CR1−FKN binding reaction was analyzed using the spinning disk by comparison of parental 300-19 cells, which do not express CX3CR1- and CX3CR1-transfected 300-19 cells and CR3CR1-transfected 300-19 cells with and without FKN (Figure 4A). The background τ_{50} values of 4.1 and 4.9 dynes/cm^2 represent the nonspecific binding and were less than 10% of the specific adhesion values.

To determine the K_{2D} for CX3CR1 on transfected 300-19 cells and substrate-bound FKN, τ_{50} was measured as a function of ligand density using the spinning disk device.

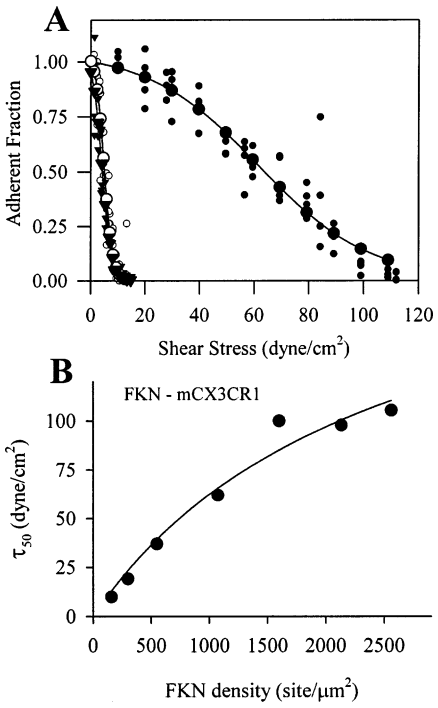

FIGURE 4: Analysis of CX3CR1-mediated cell adhesion to FKN. (A) Adhesion strength and specificity of FKN-mediated cell adhesion. Shown are the detachment profiles of nontransfected 300-19 cells plated on 0.5 μg/mL FKN (▼, $\tau_{50} = 4.9$, $R^2 = 0.89$) and mCX3CR1-transfected cells in the presence (●, $\tau_{50} = 61.8$, $R^2 = 0.91$) and absence (○, $\tau_{50} = 4.1$, $R^2 = 0.94$) of FKN. (B) Two-dimensional binding analysis of CX3CR1 to surface-bound FKN. τ_{50} was measured using a spinning disk as shown in panel A using 300-19 (CX3CR1) cells for different levels of bound FKN. The data were fit to a single-site saturation binding using the SigmaPlot ligand binding program. The FKN density was determined from the binding data in Figure 3. $K_{2D} = 2488 \pm 1042$ site/μm^2, $R^2 = 0.97$, $n = 3$.

Figure 4B shows the values for τ_{50} plotted as a function of ligand density. As shown above, these values were obtained when the binding reaction was at equilibrium. Several additional conditions are required for interpretation of this binding data. (i) There must be only one population of receptors. This is shown in Figure 4A since the nontransfected cells show only background levels of binding. (ii) Binding must not be cooperative. There is no evidence for this in FKN−CX3CR1 binding. (iii) There must be a sufficient excess of ligand at all densities. The CX3CR1-transfected 300-19 cells have a cell radius of about 3 μm and express about 10^5 receptors/cell (see below), which gives a maximum surface density of 10^3 receptors/μm^2. [Note that the total surface is about twice the surface of the sphere; hence, actual receptor densities could be reduced by a factor of 2 (*3*).] The plot in Figure 4B extends just over the K_{2D} for the binding reaction. Because K_{2D} represents the point at which 50% or 5×10^2 receptors were bound for a ligand density of $3.2 \times 10^3/\mu$m^2, there was a >5-fold excess of ligand at all points on the curve. A 5-fold excess is sufficient to prevent any major distortion of the data (*27*). Thus, the basic assumptions of the model are met, and the curve fit in Figure 4B can be used to estimate the value for the K_{2D} for the CX3CR1−FKN bond. The value obtained for K_{2D} from the curve fit was $2.5 \times 10^3/\mu$m^2 (Table 1). The major limitation in this measurement stems from the inability to achieve ligand densities much above K_{2D} for the reaction.

Quantitative Analysis of a 2D Binding Constant for CXCR1. To test the generality of this binding analysis, similar analyses were performed using CXCR1, which is another 7-transmembrane G-protein-coupled receptor (*28*). Its normal ligand is IL-8, which is not normally produced in a membrane-bound form. To extend the principles demonstrated for CX3CR1, a form of IL-8 was constructed in which the receptor binding domain of IL-8 was spliced onto the 6-His-tagged mucin-rich stalk from FKN. The 300-19 cells were transfected with a construct expressing CXCR1. This provided the means to construct an IL-8 substrate directly analogous to the FKN substrate described above and to apply the same principles with the spinning disk to analyze the number of receptor−ligand bonds in the 2D configuration. Figure 1A shows the cell surface expression of CXCR1 on the transfected 300-19 cells. Figure 5A shows the adhesion profiles for parental 300-19 cells and 300-19 cells expressing CXCR1, demonstrating both that the analytic method can be applied to this receptor−ligand combination and that the reactions are receptor and ligand specific. Figure 5B extends the specificity analysis by examining the binding of both CXCR1 and CX3CR1 to both FKN and IL-8 ligands. There was no detectable cross-reactivity between the receptor−ligand pairs.

Figure 5C shows the analysis of τ_{50} using the spinning disk device as a function of IL-8 density and parallels the results shown in Figure 4B for CX3CR1 and FKN. The value for K_{2D} calculated from this analysis was $8.6 \times 10^2/\mu$m^2 (Table 1). In this case, half of the measured points were $> K_{2D}$. This provides a strong demonstration that this form of analysis can be applied to the determination of 2D binding constants and overcomes the limitation shown in the analysis of the CX3CR1−FKN measurements imposed by the maximum practical ligand density achieved.

Comparison of 2D and 3D Ligand Binding Parameters and Bond Strength for CXCR1 and CX3CR1. The K_{3D} for binding of soluble FKN to cells expressing CX3CR1 and for the binding of IL-8 to CXCR1 is to be in the 0.8−4 nM range (*22*, *29*, *30*). To provide a comparison between the FKN and the IL-8 binding in 2D vs 3D, we analyzed the K_{3D} for each. The 6-His-tagged mucin stalk FKN and IL-8 constructs were labeled with iodinated Boulton−Hunter reagent and used in binding experiments to the CX3CR1 and CXCR1 expressing cells, respectively (Figure 6). The binding of labeled ligand to parental 300-19 cells was used as the negative control. The values of K_{3D} that were calculated from the binding plots curve fits were similar to the previous reports (Table 1). The binding data shown in Figure 6 were also used to calculate the total number of receptors per cell based on eq 1 (B_{max}).

To provide a basis for comparison of K_{2D} and K_{3D}, it is necessary to convert the K_{2D} density to concentration. This can be done by assuming a cell substrate separation distance of 20 nm. This is consistent from analyses using interference reflection microscopy (data not shown). K_{2D} (the ligand density necessary to bind 50% of the CX3CR1 receptors) was determined to be $2.5 \times 10^3/\mu$m^2 (Table 1) or, given the 20 nm separation distance, 2.1×10^{-4} M. Comparing this to the value for K_{3D} of 3×10^{-9} M gives a 6.9×10^4-fold difference. This difference in affinity was not expected and indicates that even for receptors with relatively low K_{3D} values, only a minor portion may be occupied when the

Table 1: Two- and Three-Dimensional Binding Parameters

		2D ± SEM		3D ± SEM		
receptor	ligand	K_{2D} (μm^2)	R^2	K_{3D} (nM)	R_T	R^2
CX3CR1	FKN	2488 ± 1042	0.97	3.06 ± 0.81	1.08 ± 0.11 × 10^5	0.98
CXCR1	IL-8	863 ± 273	0.95	1.54 ± 0.14	2.21 ± 0.05 × 10^5	0.99

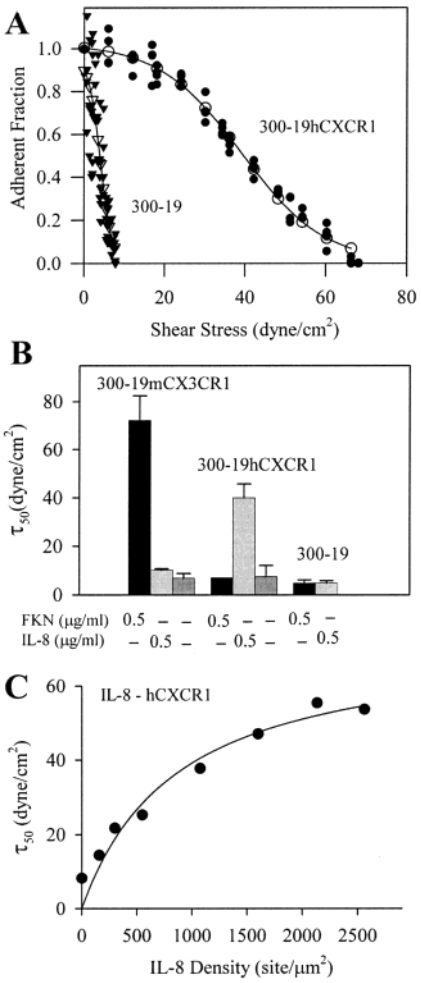

FIGURE 5: Analysis of CXCR1-mediated cell adhesion to IL-8. (A) Detachment profiles of nontransfected (τ_{50} = 4.1, R^2 = 0.94) and hCXCR1-transfected (τ_{50} = 39.1, R^2 = 0.98) 300-19 cells on 0.5 μg/mL 6-His-tagged IL-8−mucin stalk chimera-coated surface using the spinning disk assay. (B) Comparison of adhesion strength and specificity of binding of CX3CR1−FKN and CXCR1−IL-8. Shown are the combined data from three independent experiments with the mean adhesion strength (τ_{50}) and standard error. (C) Two-dimensional binding analysis of CXCR1 to varying densities of surface-bound IL-8 using the spinning disk analysis. The IL-8 density was assumed to be the same as that for FKN shown in Figure 3 because of the similarity of the constructs. K_{2D} = 863 ± 273 site/μm^2, R^2 = 0.95, n = 3.

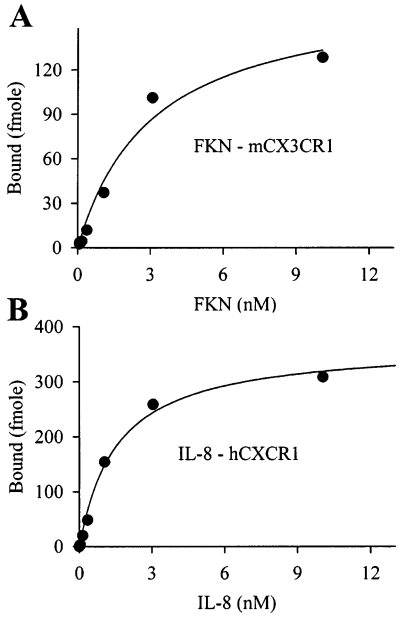

FIGURE 6: Demonstration of 3D ligand−receptor binding analyzed by radioligand binding assay. (A) Saturation binding plot for ^{125}I-FKN to 300-19 mCX3CR1 cells. (B) Saturation binding plot for ^{125}I-IL-8 to 300-19 hCXCR1. Nonspecific binding, determined using parental 300-19 cells, was <5% at each ligand concentration and was subtracted. K_D and B_{max} of each binding are calculated from a single-site saturation curve fit by the SigmaPlot ligand binding equation and summarized in Table 1.

ligand is immobilized on a surface. Interestingly, the ratio of K_{2D} to K_{3D} was similar for both receptor−ligand pairs (Table 1). This implies that the reduction in binding in the contact zone was by a similar factor for each and hence is likely to be determined by the cell type, receptor−ligand type, and cell−substrate contact zone.

Because the CXCR1 and CX3CR1 receptor systems are expressed in the same cell type and their ligands were similarly expressed on the stalk of FKN, it is possible to compare their relative bond strengths. The K_{2D} for CXCR1 was about one-third of that for CX3CR1, and the level of cell surface expression was about 2-fold (Table 1). This means that there would be 6-fold more CXCR1−IL8 bonds at the same ligand density. The mean cell detachment force was about 1.75-fold higher for CX3CR1 cells on FKN (Figure 4B). Therefore, the average CX3CR1−FKN bond would be about 10-fold stronger than the CXCR1−IL8 bond. Thus, although the CX3CR1−FKN bond has a higher K_D (lower affinity), it has a higher bond strength. This lack of correlation between bond strength and affinity implies that bond energy (RT ln $1/K_D$) is not the only determinant of bond strength.

The comparison of the two receptor−ligand bond systems also provides some important controls for the experimental conditions. The cells are held to the substrate through a linkage that includes both the receptor−ligand bond and the 6-His tag−antibody bond. In theory, either of these bonds could be the weak link that ruptures under force. The 10-fold difference in bond strength demonstrates that it must be the receptor−ligand bond that ruptures at least for the CXCR1−IL-8 bonds. Second, the K_{2D} for the CXCR1−IL-8 bond was 6-fold lower suggesting that this would come to equilibrium more rapidly than the CX3CR1−FKN bond and hence would be close to equilibrium by the 15 min assay time used above.

DISCUSSION

The data demonstrate that using a receptor−ligand pair that have nanomolar K_D values for solution binding and

concentrating the receptor and ligand in a cell−substrate contact zone require a surprisingly high ligand density to achieve 50% binding of the receptor. When the ligand is immobilized, the receptors must diffuse within the membrane to interact with ligands. This process is limited by diffusion rates of the receptors in the cell membrane and by the separation distance between cell and substrate.

Previous analyses of the binding of receptors and ligands in the 2D contact zone have used either analysis of ligand concentration within the contact zone or mechanical means to measure the binding constants (*2*). The two approaches gave very different relationships between 2D and 3D binding constants. For the fluorescent method, there was little difference between the two when compared as above, but for the mechanical methods, the 2D analyses reported K_{2D} values that were 3−5 orders of magnitude greater than predicted. One explanation that has been proposed is that the fluorescent methods measured the reactions at equilibrium whereas most of the mechanical analysis involved the measurement of single or a very small number of bonds under nonequilibrium conditions (*2*). The analyses performed here appear to be close to equilibrium and involve a large number of bonds, so this is not consistent with the previous interpretation. The other difference between the two approaches is that in the fluorescent localization method, there is an assumption that the distribution into the contact zone is equivalent to binding. The data presented here show that many of the receptors in the contact zone are not bound and hence that assumption would not be valid for the chemokine receptor−ligand system analyzed here. The second important difference for the fluorescence localization method is that the ligand was free to diffuse in a lipid bilayer. This would produce variations in ligand density that would not apply to the immobnilized case described here. The experiments that are most directly comparable with the current analysis are the measurements of E- and P-selectin binding using a plate centrifugation assay for cell detachment (*9*). The values of K_{2D} relative to K_{3D} in those studies are in general agreement with the data presented here.

This analysis would suggest that the difference between the K_{2D} and the K_{3D} values was a property of the cell, substrate ligand, and experimental approach rather than a property of the receptor−ligand bond. In that case, the ratio of K_{2D} to K_{3D} for similar receptor−ligand types measured in homologous conditions should be constant. This relationship was not apparent from the data available in the literature probably because of differences in the cell systems and methods used (*2*). By treating both receptor−ligand systems similarly and using the same parental cell type for expression, the data presented here do show similar K_{2D}:K_{3D} ratios as predicted.

The CX3CR1−FKN receptor−ligand pair is unusual among the chemokines because FKN can be expressed as a cell surface-bound ligand (*17*, *18*). This led to the speculation that it could function in the arrest of leukocytes from flow in the circulatory system and the demonstration of this property in vitro (*20*, *31*). Unlike selectin-mediated adhesion, CX3CR1 does not induce cell rolling, only firm adhesion (*20*). This would be consistent with a larger number of receptors required for the arrest, which would reduce the probability of detachment. On the basis of the measurements presented here, it would require about 1000 receptors bound per cell to resist detachment by the 10 dyne/cm^2 shear stress that is common in large blood vessels. Because of the unexpectedly high K_{2D}, this would require surface expression levels in the range of 10^5/cell for both CX3CR1 on the leukocyte and FKN on the endothelial cell. Thus, relatively high levels of both receptor and ligand expression would be necessary to form this many bonds rapidly to mediate arrest by themselves. Alternatively, altherosclerosic plaques provide a disruption of the laminar flow patterns and would provide a context in which CX3CR1 could function as an adhesion receptor. Consistent with this speculation, knockout of CX3CR1 in mice leads to a reduction of altherosclerosis (*32*). Comparison of CX3CR1 with CXCR1 in terms of their ability to resist detachment shows that the CX3CR1 has about a 10-fold advantage in the minimal number of bonds that would be required for cell arrest. Interestingly, this increase in apparent bond strength does not appear to be accompanied by a decrease in K_D (or an increase in bond energy). Therefore, it appears that bond strength and bond energy can be determined somewhat independently through the specific molecular interactions in the receptor−ligand interface.

ACKNOWLEDGMENT

Dr. Chung Zhu (Georgia Institute of Technology) is acknowledged for helpful discussions.

REFERENCES

1. Dustin, M. L., Ferguson, L. M., Chan, P. Y., Springer, T. A., and Golan, D. E. (1996) Visualization of CD2 interaction with LFA-3 and determination of the two-dimensional dissociation constant for adhesion receptors in a contact area, *J. Cell Biol. 132*, 465−474.
2. Dustin, M. L., Bromley, S. K., Davis, M. M., and Zhu, C. (2001) Identification of self-through two-dimensional chemistry and synapses, *Annu. Rev. Cell Dev. Biol. 17*, 133−157.
3. Dustin, M. L., Golan, D. E., Zhu, D. M., Miller, J. M., Meier, W., Davies, E. A., and van der Merwe, P. A. (1997) Low affinity interaction of human or rat T cell adhesion molecule CD2 with its ligand aligns adhering membranes to achieve high physiological affinity, *J. Biol. Chem. 272*, 30889−30898.
4. Alon, R., Chen, S., Puri, K. D., Finger, E. B., and Springer, T. A. (1997) The kinetics of L-selectin tethers and the mechanics of selectin-mediated rolling, *J. Cell Biol. 138*, 1169−1180.
5. Kaplanski, G., Farnarier, C., Tissot, O., Pierres, A., Benoliel, A. M., Alessi, M. C., Kaplanski, S., and Bongrand, P. (1993) Granulocyte-endothelium initial adhesion. Analysis of transient binding events mediated by E-selectin in a laminar shear flow, *Biophys. J. 64*, 1922−1933.
6. Smith, M. J., Berg, E. L., and Lawrence, M. B. (1999) A direct comparison of selectin-mediated transient, adhesive events using high temporal resolution, *Biophys. J. 77*, 3371−3383.
7. Chesla, S. E., Selvaraj, P., and Zhu, C. (1998) Measuring two-dimensional receptor−ligand binding kinetics by micropipet, *Biophys. J. 75*, 1553−1572.
8. Zhao, H., Dong, X., Wang, X., Li, X., Zhuang, F., Stoltz, J. F., and Lou, J. (2002) Studies on single-cell adhesion probability between lymphocytes and endothelial cells with micropipet technique, *Microvasc. Res. 63*, 218−226.
9. Piper, J. W., Swerlick, R. A., and Zhu, C. (1998) Determining force dependence of two-dimensional receptor−ligand binding affinity by centrifugation, *Biophys. J. 74*, 492−513.
10. Garcia, A. J., Ducheyne, P., and Boettiger, D. (1997) Quantification of cell adhesion using a spinning disc device and application to surface-reactive materials, *Biomaterials 18*, 1091−1098.
11. Garcia, A. J., Huber, F., and Boettiger, D. (1998) Force required to break alpha5beta1 integrin-fibronectin bonds in intact adherent cells is sensitive to integrin activation state, *J. Biol. Chem. 273*, 10988−10993.

12. Lotz, M. M., Burdsal, C. A., Erickson, H. P., and McClay, D. R. (1989) Cell adhesion to fibronectin and tenascin: Quantitative measurements of initial binding and subsequent strengthening response, *J. Cell Biol. 109*, 1795−1805.
13. Garcia, A. J., and Boettiger, D. (1999) Integrin-fibronectin interactions at the cell-material interface: initial integrin binding and signaling, *Biomaterials 20*, 2427−2433.
14. Garcia, A. J., Takagi, J., and Boettiger, D. (1998) Two-stage activation for $\alpha 5\beta 1$ integrin binding to surface-adsorbed fibronectin, *J. Biol. Chem. 273*, 34710−34715.
15. Imai, T., Hieshima, K., Haskell, C., Baba, M., Nagira, M., Nishimura, M., Kakizaki, M., Takagi, S., Nomiyama, H., Schall, T. J., and Yoshie, O. (1997) Identification and molecular characterization of fractalkine receptor CX3CR1, which mediates both leukocyte migration and adhesion, *Cell 91*, 521−530.
16. Combadiere, C., Salzwedel, K., Smith, E. D., Tiffany, H. L., Berger, E. A., and Murphy, P. M. (1998) Identification of CX3CR1. A chemotactic receptor for the human CX3C chemokine fractalkine and a fusion coreceptor for HIV-1, *J. Biol. Chem. 273*, 23799−23804.
17. Bazan, J. F., Bacon, K. B., Hardiman, G., Wang, W., Soo, K., Rossi, D., Greaves, D. R., Zlotnik, A., and Schall, T. J. (1997) A new class of membrane-bound chemokine with a CX3C motif, *Nature 385*, 640−644.
18. Pan, Y., Lloyd, C., Zhou, H., Dolich, S., Deeds, J., Gonzalo, J. A., Vath, J., Gosselin, M., Ma, J., Dussault, B., Woolf, E., Alperin, G., Culpepper, J., Gutierrez-Ramos, J. C., and Gearing, D. (1997) Neurotactin, a membrane-anchored chemokine upregulated in brain inflammation, *Nature 387*, 611−617.
19. Juliano, R. L. (2002) Signal transduction by cell adhesion receptors and the cytoskeleton: functions of integrins, cadherins, selectins, and immunoglobulin-superfamily members, *Annu. Rev. Pharmacol. Toxicol. 42*, 283−323.
20. Haskell, C. A., Cleary, M. D., and Charo, I. F. (1999) Molecular uncoupling of fractalkine-mediated cell adhesion and signal transduction. Rapid flow arrest of CX3CR1-expressing cells is independent of G-protein activation, *J. Biol. Chem. 274*, 10053−10058.
21. Key, T. A., Bennett, T. A., Foutz, T. D., Gurevich, V. V., Sklar, L. A., and Prossnitz, E. R. (2001) Regulation of formyl peptide receptor agonist affinity by reconstitution with arrestins and heterotrimeric G proteins, *J. Biol. Chem. 276*, 49204−49212.
22. Haskell, C. A., Cleary, M. D., and Charo, I. F. (2000) Unique role of the chemokine domain of fractalkine in cell capture. Kinetics of receptor dissociation correlate with cell adhesion, *J. Biol. Chem. 275*, 34183−34189.
23. Garcia, A. J., Vega, M. D., and Boettiger, D. (1999) Modulation of cell proliferation and differentiation through substrate-dependent changes in fibronectin conformation, *Mol. Biol. Cell 10*, 785−798.
24. Grinnell, F., and Feld, M. K. (1981) Adsorption characteristics of plasma fibronectin in relationship to biological activity, *J. Biomed. Mater. Res. 15*, 363−381.
25. Underwood, P. A., Steele, J. G., and Dalton, B. A. (1993) Effects of polystyrene surface chemistry on the biological activity of solid-phase fibronectin and vitronectin, analysed with monoclonal antibodies, *J. Cell Sci. 104*, 793−803.
26. Iuliano, D. J., Saavedra, S. S., and Truskey, G. A. (1993) Effect of the conformation and orientation of adsorbed fibronectin on endothelial cell spreading and the strength of adhesion, *J. Biomed. Mater. Res. 27*, 1103−1113.
27. Lauffenburger, D. A., and Linderman, J. J. (1993) *Receptors: Models for Binding, Trafficking, and Signaling*, pp 19−34, Oxford University Press, New York.
28. Murphy, P. M., Baggiolini, M., Charo, I. F., Hebert, C. A., Horuk, R., Matsushima, K., Miller, L. H., Oppenheim, J. J., and Power, C. A. (2000) International union of pharmacology. XXII. Nomenclature for chemokine receptors, *Pharmacol. Rev. 52*, 145−176.
29. Baggiolini, M., Dewald, B., and Moser, B. (1997) Human chemokines: an update, *Annu. Rev. Immunol. 15*, 675−705.
30. Inglese, J., Samama, P., Patel, S., Burbaum, J., Stroke, I. L., and Appell, K. C. (1998) Chemokine receptor−ligand interactions measured using time-resolved fluorescence, *Biochemistry 37*, 2372−2377.
31. Fong, A. M., Robinson, L. A., Steeber, D. A., Tedder, T. F., Yoshie, O., Imai, T., and Patel, D. D. (1998) Fractalkine and CX3CR1 mediate a novel mechanism of leukocyte capture, firm adhesion, and activation under physiologic flow, *J. Exp. Med. 188*, 1413−1419.
32. Lesnik, P., Haskell, C. A., and Charo, I. F. (2003) Decreased atherosclerosis in CX3CR1-/-mice reveals a role for fractalkine in atherogenesis, *J. Clin. Invest. 111*, 333−340.

BI0362121